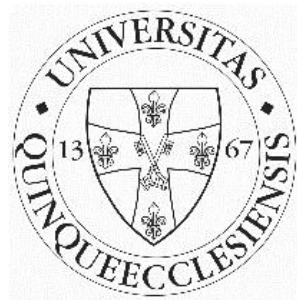


Molecular pathology of renal tumors with embryonal origin

Doctoral (PhD) theses

Author: Dániel Bányai M.D.



Department of Urology

Medical School, University of Pécs

Pécs, 2019

Head of the Doctoral School: Prof. Gábor Kovács L., M.D., Ph.D.,D.Sc.

Program leader: Prof. László Pajor, M.D., Ph.D.,D.Sc.

Project leaders: Prof. Gyula Kovács, M.D., Ph.D.,D.Sc.

1. Introduction

In 1882 Cohnheim postulated that “ein Fehler, eine Unregelmässigkeit der embryonalen Anlage ist, in der die eigentliche Ursache der späteren Geschwulst gesucht werden muss”, e.g. an error and impaired regulation in embryonic „Anlage“ may later lead to tumor development. „Aber was wir als angeboren verlangen, ist ja nicht die Geschwulst, sondern lediglich die Anlage dazu, d.h. nach der von uns proponirten Formulirung die Existenz desjenigen über das physiologische Maass hinaus producirten Zellenquantum, aus dem eine Geschwulst sich entwickeln kann“ e.g. we expect the new-born to bring not the tumor itself, but merely the superabundant cell material into the world, from the latter a tumor may develop.

The development of kidney underlies a complex molecular genetic process involving several signal transduction pathways. The temporary and spatial expression of genes, the changing gradient of proteins within the emerging structures control the differentiation of approximately 25 functionally and morphologically distinct cells of the nephron and the stroma. Termination of nephrogenesis and differentiation of specialized cell types along the nephron is a well-coordinated molecular process. Taking into account the finely tuned relationship between growth- and differentiation controlling signals, changes (e.g. mutation or altered gene dosage of any genes involved) may disturb the balance and favor cell proliferation and inhibit the terminal differentiation. To produce the appropriate number of cells for development of approximately 200 thousand to 2 million nephron, cells in the renewing blastemal niche undergo a forced mitotic activity resulting in variable level of errors, e.g. in an embryonal genetic noise.

The disturbance of embryonal differentiation may lead to inborn developmental syndromes such as CAKUT (congenital anomalies of the kidney and urinary tract). In this relation might be interesting to notice that 40% of renal functional failure in childhood is associated with CAKUT. It is not surprising that several differentiation error is associated with pre-neoplastic lesions and tumors. Wilms' tumor (WT) has already been recognized as a useful model to explore tumor development from “not differentiated superabundant” embryonic rest cells, e.g. nephrogenic rests (NR) as proposed by Cohnheim in 1882. Molecular genetic studies confirmed the connection between WT and impaired differentiation during kidney development. Several genes which are expressed spatially and temporally during early nephrogenesis, especially during the mesenchyme to epithelium transition (MET), have already been implicated in the molecular biology of WT.

Nearly 25 years ago it was suggested that papillary renal cell tumor (PRCT) of adults may also arise from nephrogenic rest-like lesions. During our work on the thesis, we have recognized that another tumor of adults, the so called mucinous tubular and spindle cell carcinoma (MTSCC) is associated with NR-like lesions. These findings suggest that not only the WT but also some tumors of adults may originate from not differentiated embryonal rest cells. The origin of a rare occurring tumor of adults, the metanephric adenoma (MA) is not yet known.

It is well documented that WT, PRCT, MTSCC and also MA may have overlapping histology. The solid, tubular or tubular-papillary growth of small epithelial-like cells in WT may pose a differential diagnostic problem, especially when the WT occur in young adults. The so-called atypical MA may also display tubular and tubular-papillary structures pure epithelial WT. Although, most MTSCC show mucinous stroma and

fibroblast-like cells, several of them may have solid-tubular-papillary growth pattern of medium-sized epithelial cells without mucinous stroma. The small cell form of PRCT, especially the papillary adenoma may also display solid-tubular growth pattern. The overlapping morphology may the diagnosis of several cases uncertain. Although the genetic analysis discriminates WT, MA, MTSCC and PRCT unequivocally, pathologist restrain to H&E morphology and immunohistochemistry. Unfortunately, we do not have biomarkers to discriminate the aforesaid tumors with overlapping phenotype.

2. Objectives

It is well known from the literature that WT develops from not differentiated nephrogenic rests. However, opinions on the development and origin of MA, MTSCC and PRCT are controversial.

To clear the correlation between embryonal rests and tumors of embryonal origin we carried out the following analysis:

- 2.1. Immunohistochemistry of WT and associated precursor lesions,
- 2.2. Histological variations and immunohistochemistry of genetically unequivocally identified MA,
- 2.3. Histological variations and immunohistochemistry of genetically unequivocally identified MTSCC and associated precursor lesions,
- 2.4. Histological variations and immunohistochemistry of genetically unequivocally identified PRCT and their precursor lesions,
- 2.5. Immunohistochemistry of genes expressed timely and spatially during kidney development.

3. Materials and Methods

3.1. Tissue samples.

We have included 12 tri- or biphasic WT, including 4 with MA-like areas, and 3 WT with blastemal predominant histological pattern. Ten MAs, 9 MTSCCs and 76 papillary RCTs, including 18 cases with solid or solid-tubular growth pattern of small “blue cells”, were also subjected to immunohistochemistry. We have also analysed 9 PLNR, 4 and 10 PNL associated with WT, MTSCC and PRCC, respectively. Original paraffin blocks of 3 foetal and 3 adult kidneys, WT, MA, MTSCC, PLNR and PNL as well as a tissue microarray (TMA) containing multiple core biopsies of 76 PRCT were used for this study.

To find pre-neoplastic lesions, we have included 14 kidneys with sporadic PRCTs (M:F=13:1) and 14 kidneys with CRCCs (M:F=9:5) in detailed histological analysis. Each kidney was cut in 3 mm thick slices and embedded in paraffin. From one of the MTSCC cases both kidneys were available for histology, both were embedded completely in 47 and 67 paraffin blocks. Three to five consecutive slides per paraffin block were stained with hematoxylin and eosin. Each slide was scored for parenchymal lesions twice.

3.2. DNA isolation

High molecular weight DNA was isolated from frozen tissues of two MTSCCs by phenol/chloroform treatment after proteinase K digestion. In the 5 cases DNA was isolated from formalin fixed and paraffin embedded (FFPE) samples.

3.3. Microsatellite analysis.

Genomic DNA extracted from normal and tumor tissue samples were subjected to PCR-based amplification of microsatellite loci using flanking primers. Four multiplex reactions included primers for amplification of all loci (multiplex #1: D3S1358, D18S51, D21S11; multiplex #2: TPOX, FGA, D5S818, D7S820, D13S317, PentaE, D16S539; multiplex #3: D1S1656, D8S1179, D10S1248, D12S391, D19S433, D22S1045; multiplex #4: D1S214, D1S2799, D9S157, D9S201, D9S1748). Electrophoresis and detection of fluorescently labeled PCR products was performed on a LI-COR 4300 DNA fragment analysis system.

3.4. DNA array based CGH.

The high molecular genomic DNA was hybridized to a 105k microarray platform, whereas the DNA extracted from FFPE tissues was subjected to 44k CGH microarray platform (Agilent Technologies), according to the procedure of manufacturer's version 5.0. Scanning and image analysis were carried out on a DNA Microarray Scanner (Agilent), according to the user's guide (version 2.0 or 5.0). The Agilent Scanner Control software (version 7.0) was used for the 5 μ m scan resolution with 100% PMT for both channels. Feature Extraction Software (version 9.5) was used for data extraction from raw microarray image files using grid template AMADID 014950 for 44k arrays and AMADID 014950 for 105k arrays. To visualize, detect, and analyze chromosomal patterns within the microarray profiles CGH Analytics Software (Agilent Technologies) was used. Global ADM 2 algorithm with a threshold 6.0 and aberration filter defaulted for minimum 3 probes in region was applied for the analysis.

3.5. Tissue microarray (TMA) construction

Paraffin blocks of fetal and adult kidneys and paraffin blocks of papillary RCCs were used for construction of TMA. From tumors with areas of different morphology and/or grade two to four

biopsies were taken. The TMA was constructed by Professor Kovacs using a Manual Tissue Arrayer (MTA1, Beecher Instruments, Inc., Sun Prairie, USA) and 0.6 mm core biopsies.

3.6. Immunohistochemistry.

For IHC staining 4µm sections placed onto FLEX IHC microscope slides (DAKO, Glostrup, Denmark) were dewaxed in xylene and rehydrated in graded ethanol. Antigen retrieval was performed through boiling the slides in 10 µM sodium citrate buffer, pH 6.0 or TE-buffer pH9 in 2100-Retriever (Pick-Cell Laboratories, Amsterdam, The Netherlands). Endogenous peroxidase activity and nonspecific staining were blocked by incubation with 3% hydrogen peroxide containing 1% normal horse serum for 10 minutes at room temperature. Slides were then incubated overnight at 4°C in moist chamber with the primary antibody at the dilution suggested by the supplier or tested in our laboratory. HRP conjugated anti-rabbit secondary antibody (MACH4 Universal HRP-Polymer, Biocare Medical, Concord, CA, USA) was applied for 30 minutes and colour was developed using DAB or AEC substrate (DAKO). Tissue sections were counterstained with Mayer's hematoxylin (DAKO) and cover-slipped with Pertex (Medite GmbH, Burgdorf, Germany) or Paramount (DAKO). In negative controls, the primary antibody was omitted. The results were evaluated by scoring as negative or positive, the latter classified according to the percentage of positive cells.

We used the following antibodies:

rabbit polyclonal anti-MET antibody (sc-12, Santa Cruz Biotechnology, Inc.) at dilution of 1:100.

rabbit polyclonal anti-HNF1B antibody (HPA-002083, Sigma Aldrich, Inc.), at dilution of 1:100;

mouse monoclonal anti-*KRT7* antibody (OV-TL, M7018, DAKO), at dilution of 1:3000;

rabbit polyclonal anti-*p504S/AMACR* antibody (13H4, RM-9130-A, Thermo-Scientific), at dilution of 1:150;

mouse monoclonal anti-*CD57* antibody (NCL-NK1, Leica Novocastra), at dilution of 1:100 hígításban;

mouse monoclonal anti-*WT1* antibody (6F-H2, M3561, DAKO), at dilution of 1:100;

rabbit polyclonal anti-*IRX1* antibody (NBP1-83090, Novus Biologicals), at dilution of 1:200;

rabbit polyclonal anti-*POU3F3* antibody (18999-1-AP, Proteintech), at dilution of 1:200.

4. Results and discussion

4.1. Differential diagnosis of tumors of embryonal origin

We describe here the immune profile of tumors which are considered to be derived from embryonal remnants. Result of immunohistochemistry of tumors as well as the associated precursor lesions is summarized in Table 1. The B3GAT1 gene product CD57 has been proposed to be a reliable marker for MA. In our study not only MA but also WT, MTSCC and PRCT showed a strong reaction with CD57 antibody, albeit in different percentage of tumor cells. The epithelial components of WTs with MA-like structures have also displayed positive staining for CD57. Our findings confirm the results of two other studies reporting CD57 positivity in MA, WT and PRCT as well. The positive CD57 staining in all types of tumor and their precursor lesions exclude CD57 as marker for MA and it cannot be used to clear its possible cellular origin.

WT1, KRT7 and AMACR antibodies differentiated between two groups of tumors and their precursor lesions (Table 1). The WT1 antibody showed a positive immune reaction in 12 of 15 WT, in all perilobar nephrogenic rests (PLNR) and MA, whereas none of the 9 MTSCC, 76 PRCC and associated pre-neoplastic lesions (PNL) displayed nuclear staining with WT1. The second group includes MTSCC and PRCT as well as their PNL, all being positive for KRT7 and AMACR. Our data are in line with previous observations showing that both PRCT and MTSCC are positive for KRT7 and AMACR whereas epithelial predominant WT and MA is positive for WT1. Our study revealed that SCEL immunohistochemistry can differentiate between MTSCC and PRCT and associated PNL as well. Within the first group of tumors CDH17 antibody differentiated between WT and MA. All but one MA, but none of the 15 WT expressed the CDH17 protein. Surprisingly, each of the 9 PLNR associated with WT was positive for CDH17 indicating an overlapping phenotype of MA and PLNR (Table 1).

Table 1. Immunohistochemistry of WT, MA, MTSCC, PRCT and associated pre-neoplastic lesions.

| Antibody | WT | | MA | MTSCC | | PRCT | |
|----------|------------|--------------|--------------|------------|------------|--------------|---------------|
| | PL-NR | T | | PNL | T | PNL | T |
| CD57 | 9/9 | 12/15 | 10/10 | 4/4 | 7/9 | 10/10 | 56/76 |
| KRT7 | 0/9 | 0/15 | 0/10 | 3/4 | 6/9 | 7/10 | 57/76 |
| AMACR | 0/9 | 0/15 | 0/10 | 2/4 | 8/9 | 7/10 | 74/76 |
| SCEL | 0/9 | 0/15 | 0/10 | 0/4 | 0/9 | 13/19 | 87/114 |
| WT-1 | 9/9 | 12/15 | 10/10 | 0/4 | 0/9 | 0/10 | 0/76 |
| CDH17 | 9/9 | 0/15 | 9/10 | 0/4 | 0/9 | 0/10 | 2/76 |

PL-NR, perilobar nephrogenic rest; T, tumour; PNL, pre-neoplastic lesion;

4.2. Precursor lesions associated with WT, MTSCC and PRCT

It was an important observation to estimate the origin of WT, MTSCC and PRCT that we found similar positive staining for antibodies in both the tumor tissues and corresponding precursor lesions. The WT1 antibody was positive in WT and in associated PL-NR. The KRT7 and AMACR genes were consequently expressed in MTSCC and PRCT as well as in their pre-neoplastic lesions. These observations strengthen the hypothesis that WT, MTSCC and PRC originate from pre-existing microscopic lesions of embryonal origin.

Unfortunately, we do not have a chance to analyze the entire kidney carrying MA to search for possible precursor lesions. However, we found that all MA, and surprisingly all PL-NR associated with WT, were positive with the CDH17 antibody. On the other hands, not even one of the WT displayed positive immune-reaction with the CDH17 antibody. All WT and the PL-NR, as expected, were positive with the WT1 antibody. The similar histology and also immune-profile of PL-NR and MA suggest that MA originates from persisting PL-NR.

4.3. Correlation between MA and PL-NR associated with WT

This unexpected result prompted us to analyze the expression of CDH17 and also the WT1 in developing kidneys. Fetal kidneys at gestational age of 12 weeks showed a positive staining with CDH17 only in parietal epithelium of the Bowman's capsule, but not in the proximal tubules or other structures. Kidneys of 3-6 months old infants and adults were completely negative. The WT1 was positive in cells of the proximal compartments of the S-shape body, glomerular podocytes and in some parietal cells of Bowman's capsule in kidneys of 12 weeks

old fetus. In infant and adult a strong nuclear positivity was seen in 50-70% of podocytes. The expression of CDH17 in parietal cells of the Bowman capsule was not expected because it is known to be specifically expressed in gastrointestinal tract and tumors arising from the digestive system including hepatocellular carcinoma. CDH17 gene encodes a cadherin-like protein with 7 extracellular cadherin domains and a transmembrane region but has no conserved cytoplasmic domain. It has a structural similarity to CDH16, a kidney-specific cadherin, but no expression of CDH17 was seen in adult kidneys.

The strong correlation between the immune-phenotype of PL-NR and MA is challenging. Most PL-NR consists of less differentiated small epithelial-like cells growing in solid-tubular, sometimes abortive papillary form. On the other hands, most WT is composed of epithelial cells of distinct differentiation, blastemal and stromal cells. Even from the histological structure of the two entities it is impossible that WT may differentiate into MA. The immunohistology further oppose this hypothesis. We did not find CDH17 positive cells within NA-like areas of WT, which exclude the possibility that a malignant WT could differentiate into benign MA.

Termination of nephrogenesis and differentiation of specialized cell types along the nephron is a well-coordinated molecular process controlled by several genes (19). By the S-shaped body stage, expression of WT1 is seen in proximal domain, where there is a distinct separation of cellular morphology between those cells fated to be podocytes and those forming parietal epithelial cells of Bowman's capsule. The impaired differentiation of cells of proximal domain may lead the development of PL-NR and subsequently of MA. The observation, that CDH17 is expressed in PL-NR and MA , as well as in parietal cells of the Bowman's capsule of exclusively fetal kidneys, strengthen this suggestion. The development

of diffuse tubular adenomas replacing both kidneys after a first trimester suicide attempt with aspirin also suggests that diffuse maturation arrest may lead to this alteration. “Embryonal hyperplasia of the Bowman capsular epithelium” (EHBCE) was observed in an infant with germ line WT1 mutations having progressive kidney failure. Association of EHBCE with MA has also been reported. Hughson et al. observed EHBCE in end stage kidney, which developed during remodeling of kidney structures in adults and therefore, cannot be originated from impaired cellular differentiation during nephron development. Presence of CD24 and CD133 positive cells in the epithelium of the Bowman’s capsule suggests that these cells retain their plasticity throughout life and they may be the source of regeneration of podocytes and also of EHBCE in end stage kidneys of adults.

4.4. Hypothesis: development of renal tumors of embryonal origin

We showed in this study by immunohistochemistry that different types of embryonal rest may occur in association with different types of tumors of embryonal origin. WT is known to be associated with IL-NR and PL-NR. IL-NR is arising due to the differentiation arrest at the earliest stage of nephron development, and has potential to develop different mesenchymal and epithelial structures, such as blastemal, stromal and epithelial cells of distinct cellular lineages characteristic for tri- or bi-phasic WT. The PL-NR, however, corresponding to impaired differentiation of primitive epithelial cells at a narrow window of epithelial differentiation, shows a slow but continuous growth and may arise to MA. Within a PL-NR sometimes hyperplastic lesions (HP-NR) may develop leading to epithelial form of WT. The pre-neoplastic lesions (PNL) associated with MTSCC and PRCT arise after completing the

mesenchymal to epithelial transition, and therefore their potential is limited exclusively to the development of epithelial lesions (Figure 1).

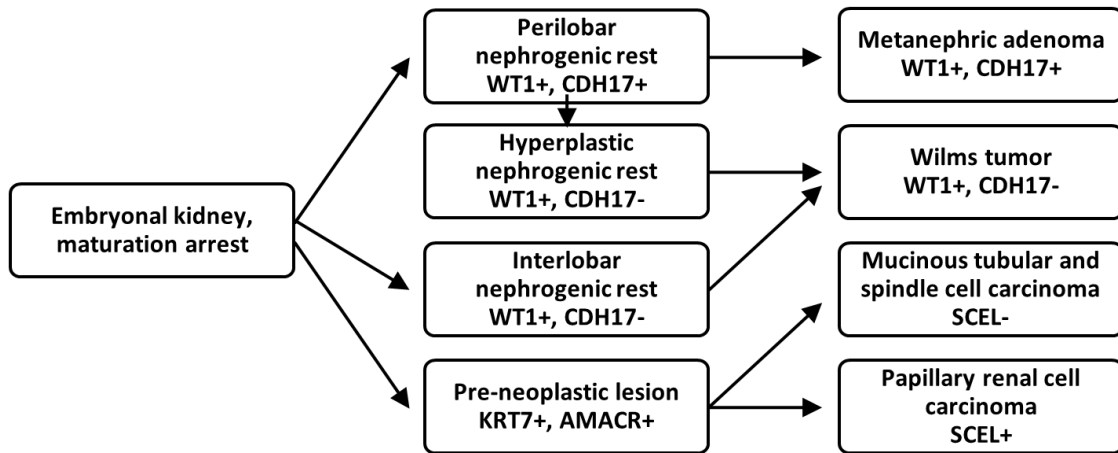


Figure 1. Proposed model for development of WT, MA, MTSCC and PRCT.

Our study clearly demonstrated that MA and PRCT are distinct entities derived from different precursors at different developmental stages of embryonal kidney. The phenotypic correlation between PL-NR and MA strongly suggests their common origin from differentiation arrested cells of the proximal domain of the S-shape body, fated to form the parietal cells of Bowman’s capsule. The finding that all WT, including those with MA-like structures were negative with CDH17 antibody excludes the possibility that MA is the hyper differentiated benign end of WT spectrum. We have confirmed the specificity of CDH17 staining in the diagnosis of MA and showed that WT1, CDH17, AMACR, KRT7 and SCEL immunohistochemistry can differentiate WT, MA, MTSCC and PRCC. The proposed model of developmental sequences for WT1, MA, MTSCC and PRCC and the involvement of different types of embryonal rest explains the origin of the aforesaid tumors.

5. Conclusions

In 1993 and 1997 there was a paradigm change in the classification of the most frequent renal cell tumors. The new classification is based on tumor specific chromosome/DNA changes which marked unequivocally conventional, papillary and chromophobe renal cancers and also the benign renal oncocytoma. Later, several rarely occurring tumors, such as MTSCC and MA, have been listed in the WHO classification. The suggested embryonal origin of PRCT has not been accepted, and the origin of MTSCC and MA has not been established.

I used the WT, the embryonal origin of which is well established, as a model to clear the origin of MA, MTSCC and PRCT. I have analyzed in this study only tumors, the diagnosis of which was established by genetic means.

The main conclusions of this thesis are the following:

A, We have confirmed the correlation between NR and WT as it was known from the literature,

B, We showed the first time that MTSCC is associated with pre-neoplastic lesions,

C, We showed the similarity between MA and PL-NR based on immune-histology for the first time,

D, We have confirmed by detailed histological analysis the strong correlation between the presence of PRCT and the large number of pre-neoplastic lesions.

E, We worked out an antibody panel suitable for differentiation of WT, MA, MTSCC and PRCT by immunohistochemistry.

F. Based on our results we propose a model for the development of WT, MA, MTSCC and PRCT from undifferentiated embryonal rest cells.

6. Acknowledgement

First of all, I would like to thank my supervisor, Professor Kovacs for introducing me in the molecular pathology of renal tumors of embryonal origin, continuously supporting me and for sharing his ideas on the topic. I am grateful to the chairman of the Urologic Clinic, Dr. Arpad Szanto allowing me to take time to work in the laboratory. My special thanks to Dr. Anetta Nagy and Professor Peter Bugert, former member of the Molecular Oncology, University of Heidelberg for allowing to use some of their results. I would like to thank Zsuzsanna Halas and Judit Szilagyi for preparing the histological slides. Thanks to the Hungarian Urological Society for generous support of my work.

And finally, my special thanks to my family for their patience and love and for the calm background for finishing my thesis.